ORGANOMETALLICS

Article

pubs.acs.org/Organometallics

Experimental and Computational Evidence for the Participation of Nonclassical Dihydrogen Species in Proton Transfer Processes on Ru−Arene Complexes with Uncoordinated N Centers. Efficient Catalytic Deuterium Labeling of H_2 with CD_3OD

Gustavo Espino,[†] Agustín Caballero,[‡] Blanca R. Manzano,[‡] Lucía Santos,[§] Mercedes Pérez-Manrique,[†] Miquel Moreno,[⊥] and Félix A. Jalón*[,‡]

[†]Departamento de Química, Facultad de Ciencias, Universidad de Burgos, Plaza Misael Bañuelos s/n, 09001 Burgos, Spain

[‡]Departamento de Química Inorgánica, Orgánica y Bioquímica, Facultad de Químicas, Universidad de Castilla-La Mancha, Avda. Camilo J. Cela 10, 13071 Ciudad Real, Spain

[§]Departamento de Química Física, Facultad de Químicas, Universidad de Castilla-La Mancha, Avda. Camilo J. Cela s/n, 13071 Ciudad Real, Spain

[⊥]Departament de Química, Edifici Cn, Universitat Autònoma de Barcelona, 08193 Bellaterra, Spain

Supporting Information

ABSTRACT: The protonation with Brønsted acids HB (HBF_4 and CF_3CO_2H) of $[RuH_2(arene)(PPh_2Het)]$ derivatives (PPh_2Het = dpim, Het = 2-*N*-methylimidazolyl; PPh_2Het = PPh_2py, Het = 2-pyridyl) that contain uncoordinated N atoms has been analyzed experimentally by NMR spectroscopy and through computational studies. Initially, at low temperature, the uncoordinated N atoms of the phosphine are protonated and a proton−hydride exchange is observed by ^1H NMR spectroscopy. The proton transfer leads to the corresponding cationic trihydride intermediates, which exhibit a dual character of classical and nonclassical hydrides, with the nonclassical species being more stable, especially when Het = 2-pyridyl. In fact, the release of H_2 and the formation of the respective monohydride complexes $[RuH(arene)(\kappa^2\text{-}N,P\text{-}PPh_2Het)]B$ was observed at room temperature. The participation of the uncoordinated N center in the proton transfer process in the stabilization of $RuH(H_2)^+$ with respect to RuH_3^+ species and in the hydride−dihydrogen exchange (cis effect) are discussed. Calculations on the complex $[RuH_3(p\text{-cymene})(PPh_3)]^+$ have also been carried out for the sake of comparison. A dual character was also found, but in this case the classical species is more stable. H/D exchange of the hydride ligands of the dihydride complexes, using CD_3OD as the deuterium source, has been studied. The very rapid deuterium labeling of H_2, catalyzed by the aforementioned dihydrides, has been observed. The known compound $[RuH_2(p\text{-cymene})(PPh_3)]$ is also active in this labeling process, and the possible mechanism for both the H/D exchange and the deuterium labeling of H_2 is discussed in light of theoretical studies.

INTRODUCTION

Protonation of transition-metal hydride complexes, L_nMH_x, with acids of different strengths is one of the most useful ways to form nonclassical dihydrogen compounds,[1] and interesting examples of classical polyhydride[2] or hydride−dihydrogen complexes[3] have been reported as products. In the majority of examples, the resulting polyhydrides[4] or hydride−dihydrogen derivatives[5] are structurally labile and exchange their positions in the metal coordination sphere.

It is widely accepted that a proton transfer process to a transition metal hydride or polyhydride follows several steps, as depicted in eq 1.[6]

$$\begin{aligned} MH + HB &\overset{(i)}{\rightleftharpoons} MH\cdots HB \\ &\overset{(ii)}{\rightleftharpoons} [M(H_2)]^+\cdots B^- \\ &\overset{(iii)}{\rightleftharpoons} [M(\eta^2\text{-}H_2)]^+ + B^- \end{aligned} \quad (1)$$

The initial interaction of the electrophilic proton of an acid, HB, with the metal hydride moiety (step i) is believed to be the first step in this process. In comparison with the direct proton transfer onto the metal center, prior attack on the hydride ligand (or on the M−H bond) has been established as kinetically more favorable in some systems.[5,7] The product of this first step is a dihydrogen-bonded complex[8] that, when sufficiently stable, can be characterized by crystallographic[9] or spectroscopic techniques such as IR and NMR.[10] As in a conventional hydrogen bond, the H···H contact involved in dihydrogen-bonded species is mainly electrostatic in nature and its formation implies the weakening of the M−H and B−H bonds. As a consequence of this contact, a downfield or upfield shift of the proton resonances for the B−H and M−H bonds, respectively, is normally observed in the ^1H NMR spectra. Additionally, a faster hydride relaxation

Received: January 6, 2012
Published: March 20, 2012

   dx.doi.org/10.1021/om300015j | Organometallics 2012, 31, 3087−3100

rate is also a consequence of the dihydrogen bond formation, an aspect that can be studied by NMR techniques. Step ii involves the full proton transfer from the conjugate base B^- to the MH bond, with the anion B^- maintaining an electrostatic contact with the coordinated H_2 molecule as an ion pair. Cases in which this intermediate has been detected spectroscopically are rare, but Shubina and others have studied several of these systems.[11] Step iii involves ion separation induced by solvation. From this dihydrogen-coordinated compound several transformation pathways are possible, depending on the electron density of the metal center. Electron-rich centers promote the oxidative addition of H_2 with or without a subsequent cis−trans MH_2 isomerization. On the other hand, in complexes with electron-poor metal centers the loss of the H_2 molecule would be possible with or without coordination of the counteranion or a solvent molecule.[12]

If the sequence of reactions in eq 1 is regarded as reversible, they would be the basis of interesting reactivity behavior—even of catalytic processes, such as hydrogen transfer, hydrogenation by heterolytic cleavage of H_2,[13] ionic hydrogenation,[14] hydrogenation of CO_2,[15] H_2 and CH labeling,[5] etc. The feasibility of designing systems with a reversible reaction sequence is not certain. However, some easy tests can be carried out to demonstrate the ability of transition-metal hydride or polyhydride derivatives to behave in such a way. Specifically, the proton−hydride exchange between the hydride coordinated to a metal and the external acid species (alcohols for instance) is considered as evidence that steps i and ii are consecutive and reversible. In addition, the labeling of H_2 with an external acid as a deuterium source can be considered as a sign that the sequence step i−step iii is reversible and that the dihydrogen coordination is labile and also reversible.

As far as the chemistry of Ru−arene polyhydride derivatives is concerned, it has been reported that the protonation of $[RuH_2(arene)(PR_3)]$ (R = alkyl, aryl) leads to trihydride Ru(IV) complexes: $[RuH_3(arene)(PR_3)]^+$.[2a,16] These compounds are now considered as classical species in analogy with the similar Os(IV)[16] and neutral cyclopentadienyl half-sandwich Ru(IV) trihydrides.[17] However, if the higher tendency of Ru vs Os and of the cationic vs neutral complexes to stabilize coordinated H_2 molecules is taken into account, some doubts emerge regarding the nature of this family of complexes.

We recently designed some systems bearing ligands with noncoordinated nitrogen centers in order to control and modify the thermodynamics and the kinetics of the proton transfer reaction.[18] These basic centers are first protonated and serve as a proton relay, transforming the proton transfer to the metal by the base into an internal sphere process[18,19] so that the intermediate structures shown in eq 1 are stabilized and can be easily studied using spectroscopic techniques.[20]

Most recently, Jiménez-Tenorio et al.[21] studied proton transfer processes starting from $[Cp^*RuH_3(\kappa^1\text{-}P\text{-}^iPr_2PCH_2X)]$ (X = pyridine, quinoline) derivatives. Experimental and computational information was compared. As previously studied by us,[18] these types of ligands are initially protonated at the heterocycle N-donor center and stabilized as conventional hydrogen-bonded (N···HA) or unconventional dihydrogen-bonded (RuH···HA) compounds when weak acids are used. With strong acids, e.g. CF_3SO_3H, such adducts are only stable at low temperature. An increase in temperature initiates a complete proton transfer process from the N*H* groups to the hydride ligands, ending in the release of H_2 and the formation of thermally stable $[Cp^*Ru(H_2)(\kappa^2P,N\text{-}^iPr_2PCH_2X)]^+$ species.

In the work described here we focus on the study of the protonation process of $[RuH_2(arene)(PPh_2Het)]$ derivatives (Het = 2-pyridyl, 2-*N*-methylimidazolyl) with HBF_4, both by experiments and with the aid of theoretical calculations. The main goal of the work was to analyze the effect of the Het moiety of the phosphines on the protonation process, more specifically the effect on (i) the reversibility of the different steps of the proton transfer process, (ii) the participation of hydrogen-bonded and nonclassical dihydrogen intermediates, and (iii) the stability of classical and nonclassical species. The possible labeling of H_2 within these species was another aim of this work. In order to elucidate the role of the acid in the overall process, we also analyzed the effect of replacing HBF_4 by CF_3CO_2H, a weaker acid that has a higher ability to coordinate its conjugated base.

RESULTS AND DISCUSSION

Preparation and Characterization of the Dihydride Derivatives. Three new η^6-arene ruthenium dihydrides of general formula $[RuH_2(\eta^6\text{-arene})(\kappa^1\text{-}P\text{-}PPh_2Het)]$ (PPh_2Het = dpim, Het = 2-*N*-methylimidazolyl, arene = *p*-cymene (**2b**), benzene (**2c**); PPh_2Het = PPh_2py, Het = 2-pyridyl, arene = *p*-cymene (**2d**)) (see Scheme 1) were prepared from the corresponding dichlorides, which had been described previously,[22] by reaction with excess KBH_4 in ethanol. For the sake of comparison, the previously known[2a] $[RuH_2(\eta^6\text{-}p\text{-cymene})(\kappa^1\text{-}P\text{-}PPh_3)]$ (**2a**) was also prepared. In the case of **2d** it was confirmed that the synthesis is also possible using an excess of $LiAlH_4$ as the hydrogen source in tetrahydrofuran (THF) (Scheme 1).

Scheme 1. Reaction Scheme for the Formation of 2a−d

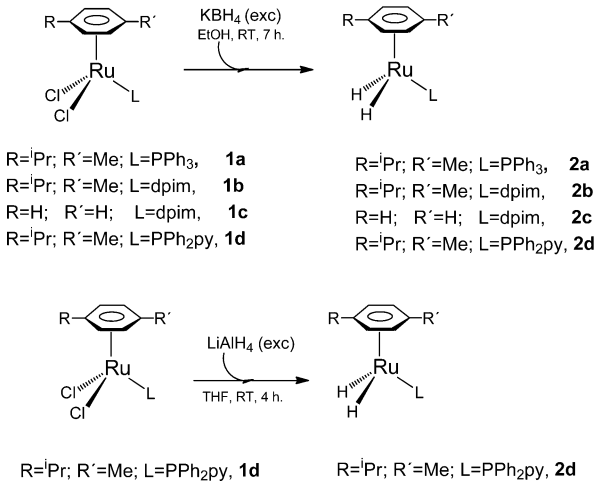

The new complexes **2b−d** are sufficiently stable to be fully characterized by elemental analysis and IR and $^{31}P\{^1H\}$, ^1H, and $^{13}C\{^1H\}$ NMR spectroscopy. 2D-NMR experiments were also carried out in order to assign all the signals.

All of the new dihydride derivatives exhibit singlets in the $^{31}P\{^1H\}$ NMR spectra (acetone-d_6), and these are at chemical shifts higher than those exhibited by their dichloride precursors: δ 52.06, 51.14, and 71.04 ppm for **2b−d**, respectively, and 7.58, 11.85, and 23.54 ppm for **1b−d**, respectively, in chloroform-*d*.

The hydride atoms give rise to one sharp doublet in the ^1H NMR spectra at about −10 ppm, and these integrate for two protons. The $^1H\{^{31}P\}$ NMR data show that the coupling is with the phosphorus atom ($^2J_{PH}$ = 40−44 Hz), and the data are also consistent with literature values for similar compounds.[2a,16]

dx.doi.org/10.1021/om300015j | Organometallics 2012, 31, 3087−3100

Protonation Experiments in an Equimolar Ratio. The reaction at room temperature of the *p*-cymene derivatives **2b,d**, dissolved in acetone-d_6, with equimolar amounts of the strong acids HB (HBF_4 and CF_3CO_2H) led to the formation of a monohydride species of general formula [RuH(η^6-*p*-cymene)(κ^2*P,N*-PPh_2Het)][B] (see Scheme 2). In this reaction, molecular hydrogen was also released, as detected in experiments with Young valve NMR tubes. These results contrast with the reported formation of trihydride derivatives [RuH_3(η^6-arene)(PR_3)][B][2a,16] (PR_3 = trialkyl, triarylphosphines) as final products after the protonation of the dihydride complexes containing PR_3 instead of the PN ligands. This difference suggests that in our family of trihydride complexes an easy access to a stable hydride−dihydrogen structure is possible. One novel aspect of this example is that this hydride−dihydrogen species would undergo substitution of the H_2 molecule by the basic N center of the phosphine. The ^{1}H NMR hydride resonances, which integrate for one H, are doublets that appear at −5.91 and −5.30 ppm for **4b,d**, respectively. In addition, the positions of all of the signals in the ^{1}H NMR spectra are modified and the resulting patterns fit best to metal-based chiral compounds with diastereotopic isopropyl methyl groups and ABCDX (X = P) spin systems for the aromatic *p*-cymene protons. Upfield-shifted singlets were observed in the corresponding ^{31}P{^{1}H} NMR spectra, at 22.32 ppm (**4b**) and 4.59 ppm (**4d**), in agreement with a chelating bidentate coordination mode for the PN ligands.[22,23]

Scheme 2. Formation of the Monohydride Species

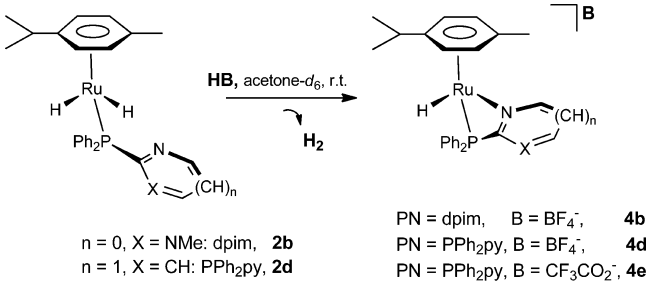

In order to shed some light on the proton transfer mechanism, we carried out the acid addition at −90 °C and monitored the proton transfer reaction from −90 to 20 °C by ^{1}H and ^{31}P{^{1}H} NMR spectroscopy. The NMR data are discussed in the following paragraphs, and the HBF_4 and CF_3CO_2H additions are covered separately.

Addition of HBF_4 to 2b or 2d in an Equimolar Ratio. The addition of HBF_4 to **2b,d** was performed, and a comparable behavior was observed in each case. Thus, the results and conclusions of both experiments will be explained together.

Initially, just after the addition of the HBF_4·Et_2O solution (equimolar amounts) at low temperature (−90 °C), a new species (**3b,d**) with ^{1}H and ^{31}P NMR resonances different from those of **4b,d** or the starting materials was observed. In the ^{1}H NMR spectra broad bands were observed at very low field: 13.40 and 12.57 ppm, respectively. These signals are assigned to N−*H* protons (see Figure 1). It can be concluded that the acid proton has been transferred to the basic sp^2 nitrogen in both coordinated ligands (dpim and PPh_2py), giving rise to the protonated derivatives [RuH_2(η^6-*p*-cymene)(κ^1*P*-PPh_2HetH)]-[BF_4] (**3b,d**) (see eq 2). New singlets were recorded in the ^{31}P{^{1}H} NMR spectra at 59.01 and 81.50 ppm for **3b,d**, respectively. Concerning the hydride resonances, the protonated compound **3b** shows, at −90 °C, an unchanged signal, in both chemical shift and resolution, with respect to the nonprotonated **2b**. In contrast, **3d** presents at this temperature a broadened signal for the hydride resonance that is shifted upfield 0.65 ppm in comparison to **2d**. This broadening and shift of the hydride resonance of **3d** can be ascribed in a first attempt to an interaction with the proton in the N*H* group, through a dihydrogen bond, that is operative in **3d** but not in **3b** at this temperature.

$$[RuH_2(\eta^6\text{-}p\text{-cymene})(\kappa^1P\text{-}PPh_2Het)] \quad (PPh_2Het = \text{dpim (2b)}, PPh_2\text{py (2d)}) \xrightarrow[-90\ ^\circ C,\ \text{acetone-}d_6]{HBF_4} [RuH_2(\eta^6\text{-}p\text{-cymene})(\kappa^1P\text{-}PPh_2HetH)][BF_4] \quad (PPh_2Het = \text{dpim (3b)}, PPh_2\text{py (3d)}) \qquad (2)$$

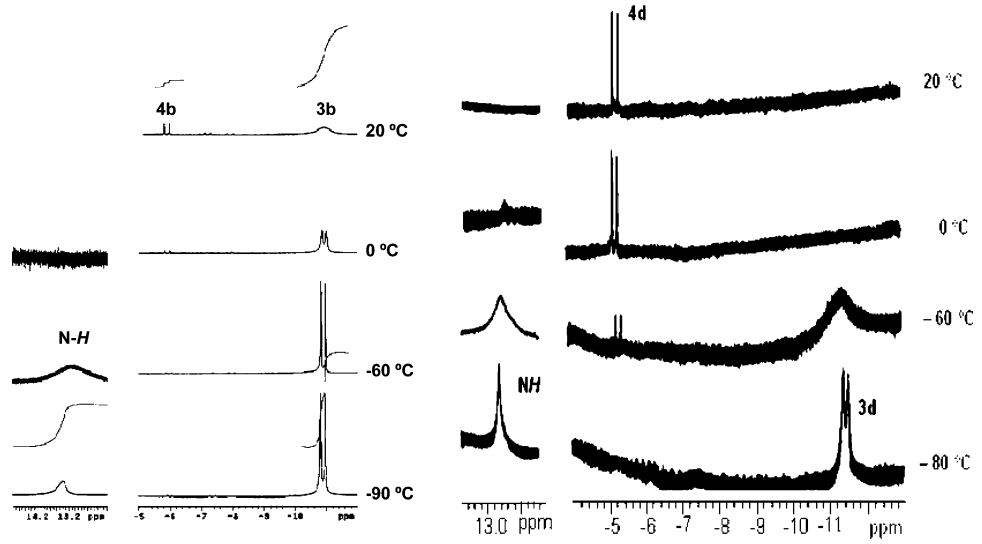

Figure 1. Evolution of high-field peaks (RuH_2, right) and low-field peaks (N−*H*, left) on increasing the temperature in the protonation experiment on **2b** (a) and **2d** (b) with HBF_4 in acetone-d_6.

dx.doi.org/10.1021/om300015j | *Organometallics* 2012, 31, 3087−3100

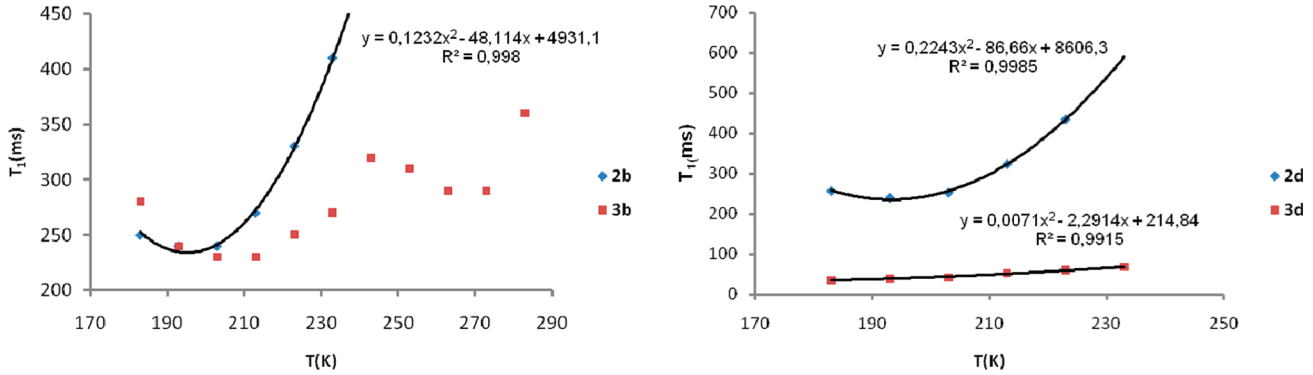

Figure 2. T_1(ms) determination as a function of temperature (K) for the hydride resonances of **2b,d** (blue sequences) and **3b,d** (red sequences) in acetone-d_6. A 300 MHz spectrometer was used.

The broadness of the N−*H* bands, for **3d** but also for **3b**, suggests that at this temperature the acidic proton is interchanging between the N atom and (probably) the BF_4^- anion, maybe as a consequence of ion pairing. The solvent, acetone-d_6, could alternatively participate in this interchange. Analogous "HBF_4 adducts" of precursors **1b,c** with the general formula $[RuCl_2(\eta^6\text{-arene})(\kappa^1\text{-}P\text{-dpimH})][BF_4]$ (arene = *p*-cymene, benzene) have been reported by our group, thus showing the ability of Ru-coordinated dpim to accept one proton.[22] Likewise, the ligand PPh_2py has been shown to favor intramolecular proton-transfer reactions after the pyridine protonation.[18a,c]

When the temperature is increased, the N−*H* resonance and the hydride doublet became broader, even for **3b**, a fact that points to a second dynamic interchange phenomenon between the two atoms (Figure 1) that is opened at lower temperature in **3d** than in **3b**. At 0 °C the broad band for the N−*H* protons had disappeared from the baseline for both compounds. The hydride resonance at 0 °C has also disappeared for **3d**, but it still appears at approximately −10.5 ppm as a broad doublet for **3b**. At 20 °C this doublet had transformed into an unresolved broad signal centered at −10.98 ppm. The position of this resonance supposes an upfield shift of 0.36 ppm with respect to the hydride signal of **2b** at the same temperature and suggests the presence of a hydrogen bond in **3b**. The coalescence temperatures for both compounds could not be determined, due to the large separation between the two resonances, but a magnetization transfer experiment confirmed unequivocally the H^+/H^- exchange. An incipient doublet at −5.91 ppm for **4b** appeared at 20 °C, whereas at −5.30 ppm the analogous signal appeared for **4d** even at −60 °C. Both of these hydride resonances integrated for one proton. These signals became more intense with time at the expense of the hydride resonances for **3b,d**.

The formation of the monohydride derivatives **4b,d** constitutes indirect evidence for the release of H_2 from an intermediate of the type $[Ru(arene)H(H_2)(PPh_2Het)]BF_4$. This coordinated dihydrogen molecule must be easily replaced by the N-donor atom of the −Het fragment.

T_1 Measurements and T_1(min) Calculations. T_1 measurements were carried out in order to provide evidence about the participation of intermediates, such as dihydrogen-bridged or nonclassical species, contributing to the hydride relaxation in the proton transfer mechanism. A 300 MHz spectrometer and the inversion-recovery method were used in all these studies.

The measurements were made at different temperatures for both the original dihydrides (**2b,d**), as reference systems, and the corresponding protonated species (**3b,d**) in order to make suitable comparisons possible (Figure 2). Different results were obtained depending on the nature of the phosphine ligand, and so each case will be discussed separately in the following paragraphs.

For the ligand dpim (pair of species **2b** and **3b**), the determination of T_1 was carried out for the hydride doublet peaks (Figure 2a). All values obtained for **3b** from 183 to 203 K are in the range of a classical hydride species and are very similar to those of **2b**, meaning that **3b** is essentially a classical dihydride in this temperature range. Nevertheless, from 203 to 243 K, a significant deviation to lower T_1 values was obtained for **3b** in comparison to **2b**. This observation, along with the unchanged chemical shift, suggests the participation of an incipient dihydrogen-bonded species. Importantly, from 243 K on, the slope of the curve that represents the T_1 values changes from positive to negative, which could indicate a more significant participation of nonclassical species at the highest temperatures studied.

With regard to ligand PPh_2py (species **2d** and **3d**), T_1 determinations were carried out on the hydride doublet for **2d** and on the N−*H* signal in the case of **3d**, since the last resonance shows fast exchange with the hydride resonance and the latter signal is too broad to record the T_1 measurement over a wide temperature range (Figure 2b). The T_1 value for N−*H* and metal−*H* groups has been demonstrated to be equal when both hydrogen atoms are in mutual exchange in a transition-metal derivative.[18c,24] In contrast to the results obtained for **3b**, T_1 values for **3d** over the whole temperature range fall within the accepted range for dihydrogen species. The minimum value is $T_{1,min}$(**3d**) = 30 ms at 161 K (extrapolated value), which is clearly lower than the value of **2d**, $T_{1,min}$(**2d**) = 240 ms at 193 K. In addition, it is possible to calculate the *d*(H−H) value for the slow rotation regime, 1.20 Å, and the fast rotation regime, 0.95 Å.[25] Both distances are in agreement with calculated values for other nonclassical hydride−dihydrogen ruthenium compounds in the literature.[26,27] Therefore, it can be concluded that **3d** can access a nonclassical $RuH(H_2)$ state even more easily than **3b**. As a comparative point with **3d**, the $T_{1,min}$ value was also determined for the N−*H* group of the chloride complex $[RuCl_2(p\text{-cymene})(PPh_2pyH)]BF_4$ (300 MHz) in acetone-d_6. The value obtained of 298 ms is very different from that of **3d**, showing the effect of the hydride on relaxation.

Considering the data presented above, there are several pieces of evidence that support the easy access to nonconventional trihydride species:

(i) the observed broadening of the hydride signals at intermediate temperatures, which suggest chemical exchange with the acidic proton through dihydrogen-bonded species

dx.doi.org/10.1021/om300015j | *Organometallics* 2012, 31, 3087−3100

(ii) the observed release of hydrogen at room temperature
(iii) the anomalous evolution of T_1 with temperature for **3b** and the low T_1 values for **3d**, which fall in the range expected for nonclassical hydride−dihydrogen compounds

The practically unaffected chemical shift of the hydride resonance in **3b,d** with respect to the corresponding dihydride precursors can be due to the similarity in the chemical shift between the involved species in the chemical exchange. In fact, the $[Ru(arene)H_3P]^+$ [2a] and $[Ru(arene)H_2P]$ species[28] reported until now exhibit very comparable chemical shifts.

The observations outlined above have several implications, and a mechanism for the whole process is proposed in Chart 1.

Chart 1

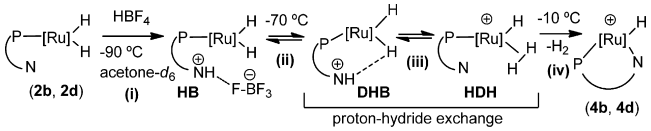

(1) At low temperature, step i involves the transfer of the acidic proton to the basic N atom. This proton is likely to be interchanged between the N atom and the BF_4^- anion (formation of a hydrogen bond, HB).
(2) The second transfer step, step ii, involves proton−hydride interactions that allow chemical exchange between the acidic proton and both hydride groups. This exchange can be explained through the participation of dihydrogen-bonded intermediates (DHB) in equilibrium with nonclassical hydride−dihydrogen species (HDH) (step iii). Both DHB and HDH are consistent with the observed decrease in the T_1 values. In the case of the DHB intermediate, a bifurcated dihydrogen-bonded structure, with the proton interacting with both hydride ligands, can also be envisaged.
(3) Finally the release of dihydrogen (step iv) yields compounds **4b,d**.

This multistep mechanism has been previously exemplified by us[18c] and Jimenez-Tenorio[21] in systems with similar phosphines coordinated to Ru. This mechanism is in contrast with the previously reported behavior of ruthenium arene trihydride derivatives of general formula $[RuH_3(arene)(phosphine)]^+$, which behave as classical hydride compounds and are stable at room temperature (hydrogen loss was not observed).[2a,16]

*Addition of HBF_4 to **2b** or **2d** in a 2:1 Molar Ratio.* We added an excess of HBF_4 to **2b** or **2d** (2:1 molar ratio). An excess of acid could lead to the possibility of stabilization of hydride−dihydrogen derivatives, since the shift of the coordinated H_2 molecule by the N-donor center could be hampered by its protonation.

Protonation with HBF_4 in a 2:1 molar ratio at very low temperature (−80 to −70 °C) gave results similar to those obtained with a 1:1 ratio (See Figure S10 in the Supporting Information). However, for mid-range temperatures (−60 to −40 °C), resonances due to the protonated species **3b,d** disappeared and several hydride doublet signals in the region 7−8.5 ppm were observed in an irreversible process. Finally, at room temperature a doublet (different from that observed for the monohydrides **4b,d**) was obtained: −7.18 ppm (J_{HP} = 54.0 Hz) for **2b** and −7.28 ppm (J_{HP} = 51.3 Hz) for **2d**. The difference in the chemical shift with respect to the hydride of **4b,d**, in conjunction with similarities in the coupling constant, may indicate a formula of the type $[RuH(p\text{-cymene})(S)(\kappa^1P\text{-}PPh_2HetH)](BF_4)_2$ (S = solvent) for these compounds, but a definitive characterization was not carried out due to a lack of stability. On the other hand, the ^{31}P NMR spectra of these final compounds, with resonances at 55.0 and 68.7 ppm for products from **2b,d**, respectively, suggest κ^1P coordination of the phosphine, and this leads to resonances very different from those found for an κ^2N,P coordination in **4b,d** (22.32 (**4b**) and 4.59 ppm (**4d**)). Similarities in the $T_{1,min}$ values of the hydride resonances (240 ms at 240 K) with those calculated for **2b,d** for these final hydride compounds also points to their classical nature. On the basis of these observations, we can conclude that, unfortunately, release of the coordinated dihydrogen is not avoided by the protonation of the N-donor centers. This finding is in contrast with the results obtained for the aforementioned protonation of $[Cp^*RuH_3(\kappa^1P\text{-}^iPr_2PCH_2X)]$ compounds, which give $[Cp^*RuH_2(H_2)(\kappa^1P\text{-}^iPr_2PCH_2XH)]$ derivatives.[21] In our opinion, the stabilization of the H_2 coordination in the cyclopentadienyl compounds may be due to the existence of a more electron-rich Ru center due to the more pronounced donor character of Cp* with respect to the *p*-cymene and the presence of two hydrides instead of one.

Computational Studies on the Proton Transfer Process. Considering the experimental evidence discussed above on the mechanism for the proton transfer reaction, we carried out a theoretical study at the DFT (B3LYP) level for the protonation of **2b** with a single H^+. The goal was to determine a reaction pathway for the proton transfer process from **2b** to **4b** and to evaluate the feasibility of the existence of nonclassical and classical polyhydride species.

The protonated compound **3b** can undergo different transformations, and these are shown in Chart 2 along with the pure electronic + nuclear energies as directly obtained from the quantum mechanical calculations. Evaluation of the zero point vibrational energy, the enthalpy energy, and the entropy term leads to the Gibbs function energies, which are also given for all the structures shown in Chart 2. Solvation energies derived from single-point calculations using a continuum model have been added to all the calculated structures.

As a reasonable starting point we chose **3b**, which—as deduced from the NMR studies—at low temperature has undergone protonation on the *N*-imidazolyl atom. Two dihydrogen-bonded minima, BF and FS1, prior to the proton−hydride exchange process were calculated that are similar in energy. BF is a bifurcated dihydrogen-bonded complex with a H···H distance (NH···HRu) around 1.94 Å, whereas in the dihydrogen-bonded FS1 the NH···HRu bond is not bifurcated, a fact that allows a smaller H···H distance of 1.78 Å. The nonbifurcated species, with a structure closer to a molecule with coordinated H_2, is better in terms of explaining the excess hydride relaxation and the proton−hydride exchange. The stated H···H distance for this interaction in FS1 is relatively large and compares well with that evaluated for other weak dihydrogen bonds such as Nb−H···HOMe[29] or ReH···HOH.[30] The stabilization due to the formation of the dihydrogen bond is small compared to that observed between alcohols and Nb[29] or Ru[31] hydrides. Given that the transformation between these three species essentially involves the rotation of the P−imidazolium bond, especially high barriers are not expected for the mutual interconversion.

Another minimum, FS2, was found for the proton transfer to the hydride atom. FS2 is a hydride−dihydrogen compound with a short H−H bond distance of 0.919 Å and with the *N*-imidazolyl atom pointing toward the transferred proton at a

dx.doi.org/10.1021/om300015j | *Organometallics* 2012, 31, 3087−3100

Chart 2. Reaction Coordinate of the Proton Transfer Process from 3b to 4b[a]

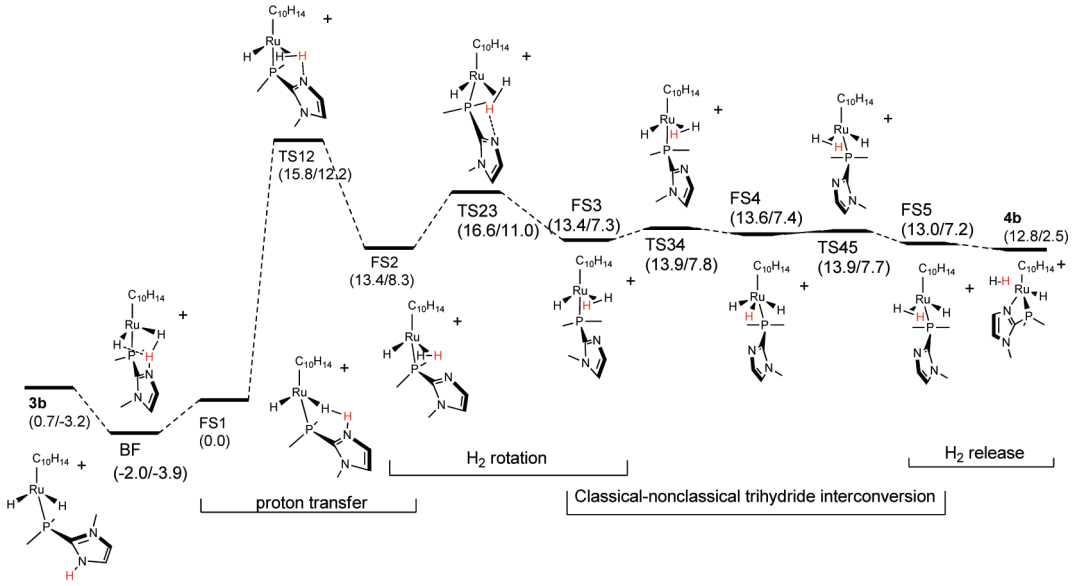

[a]Electronic (EE) and Gibbs energies (GE) in the solvent, indicated in parentheses, are in kcal mol^{-1} (EE/GE). The EE scale is represented in the chart. For a GE scale see Figure S2 in the Supporting Information.

Chart 3. (a) Fundamental and Transition States for the Proton Transfer Process in 3b–d[a]. and (b) Comparison of the Proton Transfer Process for Compound 3b with (Blue) and without (Black) the Counteranion BF_4^-[b]

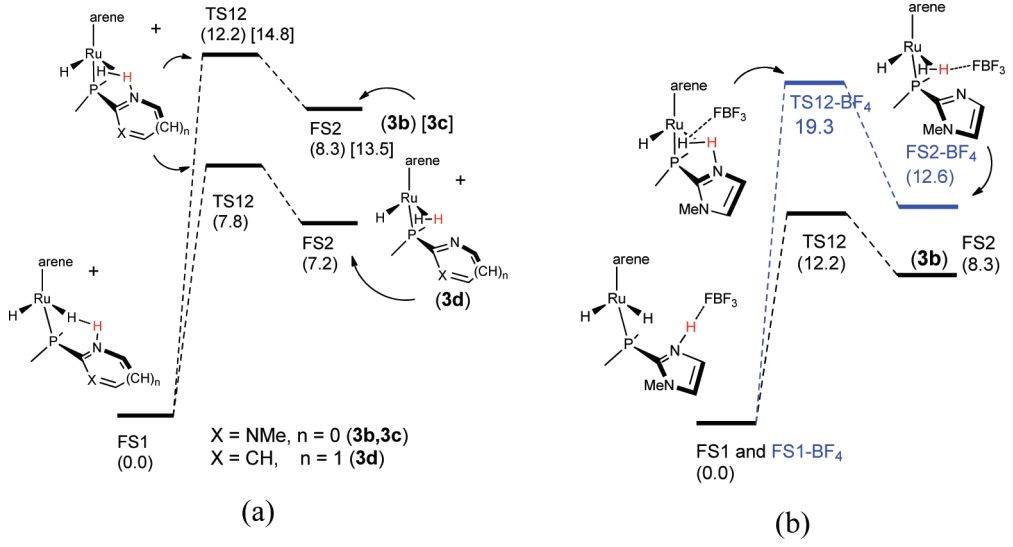

[a]Relative free energy values in the solvent (kcal mol^{-1}) are in parentheses for **3b,d** and in brackets for **3c**. [b]Relative free energy values in the solvent (kcal mol^{-1}) are given in parentheses.

distance of 2.027 Å. As a consequence, the H_2 ligand could be considered as polarized by this atom. Accordingly, the calculated Mulliken charge of the transferred proton is 0.139: i.e., higher than the value for the other H of the H_2 molecule (0.095) (Table S2, Supporting Information). We also located the transition state for the dihydrogen-bonded FS1 to the hydride–dihydrogen FS2 transformation (TS12), and the latter is 12.2 kcal mol^{-1} higher than FS1 ($\Delta G_{acetone}$ values). This value is very low compared with those found for other proton transfer reactions on transition-metal hydrides.[19,20] In our opinion this low barrier reflects the ease of this process when the proton is previously located on a basic center close to the coordination sphere of the complex.

To compare the experimental differences observed between complexes **3b** and **3d** in the accessibility to nonclassical species, the calculated energies in the proton transfer process are compared for both complexes (see Tables S1 and S3, Supporting Information). The structural parameters of the species involved are essentially the same for the two derivatives, but significant energy differences were found. A relatively lower barrier for the transition state and a lower energy for the hydride–dihydrogen FS2 minima were found for the PPh_2py derivative **3d** (see Chart 3a). This finding is consistent with the lower values of $T_{1,min}$ obtained for the derivative **3d** compared to those for **3b** and thus supports an easier access and relatively higher stability of the nonclassical species, FS2, in the case of

dx.doi.org/10.1021/om300015j | Organometallics 2012, 31, 3087–3100

the PPh_2py derivative. Calculations were also carried out on **3c**. The results are similar to those obtained for **3b** (see energy values in brackets in Chart 3a).

It is noteworthy that the process shown in Chart 3a is the key for the proton−hydride exchange and that the relative energies of the species involved confirm the reversibility of the process for these derivatives.

Chart 3b is useful for comparing the effect of the counteranion BF_4^- on the stabilization of the different structures in the proton transfer process (see Table S4 in the Supporting Information for energies and structural parameters). The introduction of the BF_4^- counteranion in structure FS1 found for **3b** involves rupture of the dihydrogen-bonding interaction in favor of proton capture by the imidazolyl moiety (FS1-BF_4), which maintains in this structure a conventional hydrogen bond with the counteranion. The second minimum in this process is FS2-BF_4. This is a hydride−dihydrogen compound with a weak interaction of one of the hydrogen atoms of the coordinated H_2 molecule with a F atom of the anion at 1.99 Å, which leads to the formation of a polarized $H-H\cdots FBF_3$ fragment. The H−H bond distance in the coordinated H_2 molecule decreases in comparison with that in the same structure without the counteranion (0.90 Å in FS2-BF_4 and 0.92 in FS2). Reinforcement of the bonding in coordinated H_2 by the effect of the counteranion has been observed previously in other systems.[24,32] A transition state (TS12-BF_4) was found between the two minima. In this structure the counteranion maintains a weak $F_3BF\cdots H$ interaction at 2.50 Å with the central hydrogen, which forms part of a coordinated H_2 molecule that interacts in turn with the N-donor center of the imidazolyl moiety at 2.01 Å. In TS12-BF_4 the H−H bond distance is 0.90 Å: i.e., markedly shorter than in TS12 (0.99 Å). As far as the relative energies of these structures are concerned, and considering FS1 and FS1-BF_4 as reference points, the activation energy of the proton transfer process increases 7.1 kcal mol^{-1} due to the effect of the BF_4^- counteranion, whereas FS2-BF_4 is destabilized by 4.3 kcal mol^{-1} due to this effect. Although the energy of other critical points in Chart 2 could also be affected by the counteranion, we have not extended our studies to other structures, because the step analyzed is the one with the highest energy barrier in the global process of proton transfer. For instance, Lledós and Basallote have recently demonstrated the influence of weak interactions of the BF_4^- anion in the rotation energy of H_2.[33]

The experimentally observed proton−hydride interchange must involve rotation of the H_2 molecule. This takes place in Chart 2 with the transformation of FS2 into FS3, also a hydride−dihydrogen complex. The corresponding transition state (TS23) was found and has a free energy barrier of 2.7 kcal mol^{-1} from FS2. It is noteworthy that the *N*-imidazolyl atom participates in this rotation as a polarizing center of the H_2 molecule. In fact, it can be seen that this basic center is always interacting with the transferred proton, shown in red in Chart 2, and this is located on the right in FS2 and at the center in TS23 and FS3. The calculated Mulliken charges of the H_2 atoms reflect the effect of this polarization, and the most positively charged hydrogen is the one that interacts with the N center (Table S2, Supporting Information).

The H−H bond distance in the H_2 molecule is shorter in TS23 (0.854 Å) than in both minima (0.919 Å). Considering that the N···H distance in TS23 is shorter (1.847 Å) than that in FS2 (2.027 Å) or FS3 (2.390 Å), it can be concluded that the H_2 molecule is elongated in the equilibrium structures—probably due to the more favorable back-donation from the Ru orbitals in this orientation (coplanar with the hydride) and to a possible interaction with the adjacent hydride ("cis effect").

The aforementioned cis effect[34] must lead to a weakening of the H_2 bond and to the consequent formation of a nascent bond between the hydride and the central hydrogen of the H_2 molecule. Covalent[34] and an electrostatic[35] mechanisms have been proposed to explain this effect. Both of these views support the proposal of Crabtree et al., in which an acid dihydrogen ligand transfers a proton to an adjacent hydride base.[36] On considering the reaction coordinate of this process from the hydride-dihydrogen complexes FS3 to FS5, we found FS4 as an intermediate and two transition states, TS34 and TS45. The H−H distances in the intermediate FS4 are long and are both very similar, 1.461 and 1.472 Å, whereas the shorter H−H distances in the respective TSs are 1.269 Å (TS34) and 1.279 Å (TS45). The H−H distances in this reaction coordinate provide conclusive evidence that FS4 is a classical trihydride structure that possibly arises as a consequence of the elongation of the H_2 bond due to the cis effect.

Evolution of the bonding pattern along the whole process can be easily tracked out by analyzing the electronic density surfaces in the $Ru-H_3$ plane and using the atoms in molecules (AIM) formalism (see Figure S5 in the Supporting Information). The presence of H−H bond critical points indicates that FS3 and FS5 are hydride−dihydrogen structures, whereas FS4 is a classical trihydride complex. The charge at the bond critical points also shows that the $Ru-H_2$ bond is weaker than the Ru−H bond (as it is usually seen) and that the H−H bond in FS3 is stronger (by ca. 0.03 au) than in FS5.

On the other hand, the three fundamental states in this process, of classical to nonclassical trihydride interconversion, fall within 0.2 kcal mol^{-1} of each other in the free energy scale and the energy profile from the classical trihydride intermediate to the hydride−dihydrogen forms is practically flat. In all five calculated structures of this reaction coordinate (from FS3 to FS5) the *N*-imidazolyl atoms point to the central hydrogen atom, indicating that this atom is the most electrophilic center in this path. This situation was further confirmed by analyzing the Mulliken charges of the hydrogen atoms bonded to the Ru center in the stated structures (see Table S2 in the Supporting Information). The relatively positive charge of the central hydrogen atom in these structures favors the mechanism driven by the cis effect on the basis of an electrostatic mechanism.[35] In relation with this statement, a relevant fact is that the electrophilic character of this central hydrogen atom is induced by the uncoordinated N center of the imidazolyl fragment. Evidence for this is provided by a comparison of the relative Mulliken charges on the H_2 molecule atoms between the $RuH(H_2)$ structures FS2 and FS3. Although both structures are very similar, the Mulliken charge is more positive for the hydrogen that interacts with the N center (Table S2) and, as stated previously, its position changes with the H_2 rotation.

At this point it is interesting to discuss our results in light of the phenomenon known as quantum mechanical exchange[37], because the cationic trihydrides $[RuH_3(arene)L]^+$ are thought to exhibit this phenomenon. Two mechanisms have been proposed, depending on the way in which the exchange coupling occurs. The first mechanism is based on the accessibility to vibrational states in the bending modes of the MH_2 unit in which the coupling exchange is observed.[38] An alternative mechanism, proposed by Limbach and Chaudret, involves the easy thermal accessibility of a hydride−dihydrogen state, $MH(H_2)$,

from a trihydride fundamental state, MH_3.[39] The same authors also proposed that when the energy barrier between these tautomers is very low, a classical exchange process (incoherent exchange) involving the scrambling of all three hydrides occurs. For many complexes that exhibit this phenomenon, the accessibility to nonclassical species has been theoretically shown to be the main parameter that governs the magnitude of the exchange coupling.[40] In our case, the very low barrier calculated supports the experimental impossibility of slowing this classical exchange down sufficiently to differentiate hydrides in an AB_2 system. This prevents the experimental determination of quantum exchange constants. Heinekey et al.[16] demonstrated that some complexes of the type $[OsH_3(arene)(PR_3)]^+$ are examples of classical trihydrides that show quantum exchange and they proposed that the analogous Ru trihydrides probably have the same property, although the low barrier for the classical exchange makes it impossible to prove this proposal. The results of our theoretical studies support the existence of a low energy barrier and the existence of the mechanism proposed by Limbach and Chaudret as the basis for the quantum exchange. However, in contrast to the findings for other similar systems, the Ru(arene)trihydride systems described here exhibit a nonclassical nature in the most stable structure, although the accessibility to classical species is easy.

It is significant that the shortest N···H distances in the structures of minimum energy (FS2, FS3, FS4, and FS5) and their TS intermediates are shorter than the sum of the van der Waals radii (2.75 Å),[41] which suggests the existence to some extent of an interaction. This situation increases the positive charge on the affected H atom and could favor the cis-effect mechanism and also reinforce the H−H bond in the coordinated dihydrogen molecule. In order to evaluate this hypothesis, the analogous structures for the classical to nonclassical trihydride interconversion (TS3 to TS5) were calculated for $[RuH_3(p\text{-cymene})(PPh_3)]^+$ (**3a**). The relative electronic energy values, considering the classical RuH_3 structures as a reference point, are shown in Chart 4. In this case ΔE and not Gibbs energies (ΔG) have been represented, since the necessary energy correction at the zero point (ZPE) would be, for some of the structures, higher in value that the differences in ΔG between the fundamental and transition states. A noteworthy conclusion we can extract from this study is that the $[Ru(arene)H_3(P)]^+$ species reported until now might be reformulated as dual classical−nonclassical species in nature.

Chart 4. Relative Energies in the Solvent (kcal mol^{-1}) for the Classical to Nonclassical Trihydride Interconversion for 3a,b, Considering the Classical Trihydride Structure (FS4) as a Reference Point[a]

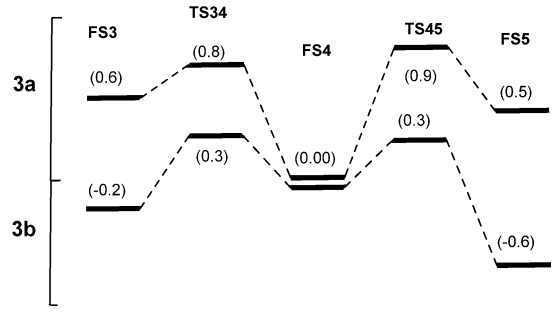

[a]See Chart 2 for the structures and the Supporting Information for selected structural parameters.

Although we do this with caution, due to the small energy differences between all these structures, the following conclusions can be drawn from Chart 4.

(1) The energy differences between classical and nonclassical species are not large for either **3a** or **3b**. However, there is a clear distinction between the two derivatives: the nonclassical species (FS3 and FS5) are the most stable ones for **3b**, whereas for **3a** the classical structure (FS4) is the lowest in energy.
(2) The H−H bond distances in H_2 (for nonclassical) and in contiguous hydride atoms (for classical) in the different species of **3b** are shorter than those in **3a**.
(3) The transition states, starting from the classical structure, are more accessible for **3b** than for **3a**.

As expected, all of these conclusions point to the polarization of the Ru−H bonds by the N-donor centers in the **3b** structures, with a consequent increase in the positive charge (see Mulliken charges in the Supporting Information). This fact increases the H_2 bond strength and, as a consequence, stabilizes the nonclassical with respect to the classical intermediates.

The final step in Chart 2 involves the release of H_2 from FS5, and this leads, through an exothermic process in the free energy scale of 4.7 kcal mol^{-1}, to the final product, **4b**.

In conclusion, the presence of an uncoordinated basic N-donor center close to the coordination sphere is important in the proton transfer process, as it stabilizes the nonclassical species, thus facilitating the proton−hydride exchange. The stabilization effect of the N-donor center on the nonclassical species is a rarely documented phenomenon, but the effects of weak bases as the counteranions on the kinetics of the deprotonation of H_2 in *trans*-$[FeH(H_2)(dppe)_2]^+$ [42] and on the relative stabilization of the nonclassical species in a cis−trans isomerization of $[W(CO)Cp^*H_2(PMe_3)_2]BF_4$ [43] have been reported. The effects on the H···H distances of stretched dihydrogen derivatives by the formation of IrCl···HIr interactions are also noteworthy.[32]

H/D Exchange and Deuterium Labeling of H_2 with 2a,b,d. Considering the easy protonation of the dihydride derivatives, the possible reversibility of the proton transfer process and the participation of hydride−dihydrogen intermediates, which could allow a hydride scrambling in the coordination sphere of the metal, we initially envisaged the study of proton−deuterium exchange in the dihydride derivatives using methanol-d_4 as the deuterium source. In addition, it has been reported that the existence of uncoordinated N-donor centers facilitates the H/D exchange.[44]

Solutions of **2b**,**d** in deuterated methanol were prepared, and their evolution with time was monitored by ^1H and $^{31}P\{^1H\}$ NMR spectroscopy. A similar study was carried out on **2a** with the aim of ascertaining whether the N-donor centers were necessary for this process to occur. The following observations were made:

(i) In all cases a decrease in the intensity of the hydride doublets was observed, a fact that reflects H/D exchange (see for instance Figures S8 and S9 for **2a** in the Supporting Information). Complete deuteration of the hydride groups was achieved for all three compounds after different reaction times and under different conditions.
(ii) The H/D exchange was slow for **2b** and faster for **2a**,**d**, but in all cases the data fit a pseudo-first-order equation

dx.doi.org/10.1021/om300015j | *Organometallics* 2012, 31, 3087−3100

best. The initial rate constants were determined at 20 °C for **2a**,**b** and at −20 °C in the case of **2d** because the process was too fast in the latter case at the higher temperature. k_{obs}(**2a**,20 °C) = 7 × 10^{-4} s^{-1}, k_{obs}(**2b**,20 °C) = 4 × 10^{-5} s^{-1}, k_{obs}(**2d**,−20 °C) = 1 × 10^{-4} s^{-1}.

(iii) The other signals in the spectra remained unchanged. Thus, the exchange process only affects the hydride atoms.

(iv) Concerning the deuterium source, only the signal of the residual OH group of the solvent increased in intensity in these experiments.

(v) RuHD isotopomers were detected in the ^1H and $^{31}P\{^1H\}$ NMR spectra, and the resonance for the RuD_2 isotopomers was also seen in the corresponding $^{31}P\{^1H\}$ NMR spectra (see Figure 3 for **2b**).

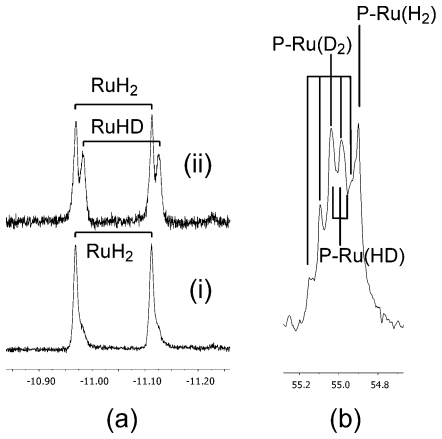

Figure 3. (a) ^1H NMR spectra of **2b** in the hydride region at 20 °C: (i) after 100 min; (ii) after 48 h. (b) $^{31}P\{^1H\}$ NMR spectrum of **2b** at 20 °C after 48 h. The resonances were assigned to the different isotopomers.

Although we initially thought that this H/D exchange process was N-mediated, the fact that **2a** shows the same phenomenon as **2b**, but even faster, suggests that other alternative mechanisms should be taken into account, at least for **2a**. Mechanistic considerations will be discussed below in light of theoretical studies.

After these experiments, it was decided to study the possible labeling of H_2 to give D_2 using methanol-d_4 as a deuterium source. This proposal is supported by the fact that this process has been demonstrated to be feasible for other dihydrogen-bonded complexes that exhibit proton−hydride exchange.[45,18a,c] In order to obtain the desired information, we used ^1H NMR spectroscopy under conditions similar to those for the previous H/D experiments to monitor the evolution of the dissolved hydrogen (after bubbling H_2 through a methanol-d_4 solution) using **2a**,**d** as catalysts. The transformation of H_2 into D_2 was quantitative after 20 min on using **2d**. In this experiment the formation of HD as an intermediate species was also observed. Compound **2a** was even more active, since only the first spectrum acquired (after approximately 5 min) showed traces of HD and these disappeared into the baseline after 5 min more. It is noteworthy that this process takes place at a much higher rate than the H/D exchange, and consequently a different pathway is expected.

The generation of D_2 from protic solvents such as CD_3OD and D_2O is a smart and environmentally friendly process that has been widely pursued in recent years. This process, which nature has solved with hydrogenases,[1b,46] is currently only available for relatively few systems.[47] Many of these applications give very low yields even under extreme conditions of temperature and pressure.

Recently, Sajiki used M/C heterogeneous catalysts (M = Pd, Pt, Rh, Ir) that were efficient in the deuteration of H_2 gas at room temperature.[48] Himeda[49] also recently reported the activity of an Ir(III) dicationic catalyst with bpy (2,2-bipyridine) type ligands. This catalyst is active in the deuterogenation of C═C and C═O bonds using D_2O as the deuterium source and H_2 or HCO_2H as hydrogenation vectors. The cationic monohydride of formula $[Cp^*Ir(H)(bipy)]^+$ is considered to be the active species.

In an effort to gain more information about possible mechanisms for the H/D exchange and the deuterium labeling of H_2, new calculations (DFT, B3LYP) were carried out, and the conclusions are graphically represented in Chart 5.

Chart 5. Reaction Coordinate for the H/D Exchange (Red Dashed Lines) and the Deuterium Labeling of H_2 (Blue Dotted Lines) from 2b in Methanol-d_4[a]

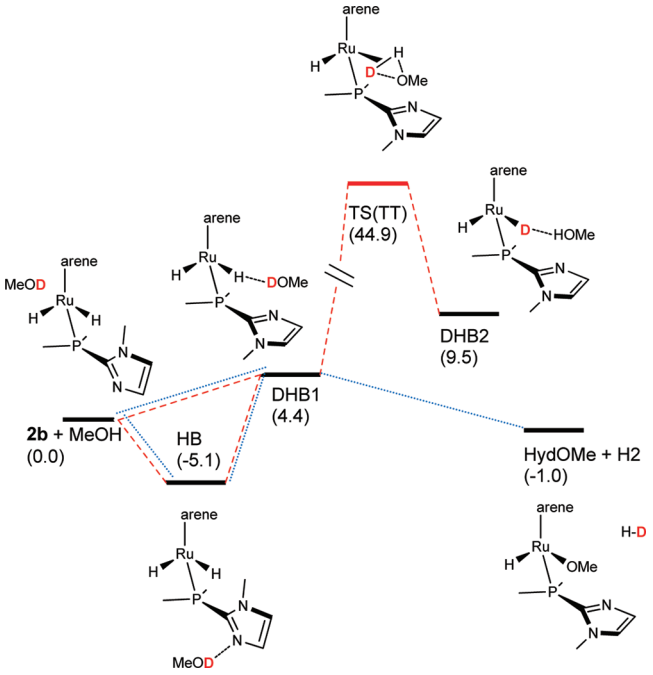

[a]Gibbs energies (GE) in methanol, indicated in parentheses, are in kcal mol^{-1}.

Complex **2b** has been chosen as starting point for this calculation. Initially **2b** reacts with a molecule of methanol to give intermediate HB, which has a conventional N···HOMe hydrogen bond with the N-donor center of the Me-imidazolyl group. Alternatively, **2b** could give DHB1, which has a dihydrogen bond (RuH···HOMe). Although HB is more stable than DHB1, the latter is also thermally accessible at 4.4 kcal mol^{-1} from the starting point. In the case of **2a** (with PPh_3) the species HB could not be formed and **2a** would be transformed into the species analogous to DHB1.

If we concentrate on the H/D exchange (red dashed lines in Chart 5), the species DHB2, analogous to DHB1 but with interchange of the H and D positions, should be formed. Between both species we have found the transition state TS(TT) that exhibits an elongated and coordinated H_2 molecule with a H−H bond distance of 1.09 Å. The oxygen atom of the MeO^-

dx.doi.org/10.1021/om300015j | Organometallics 2012, 31, 3087−3100

anion interacts with both hydrogen atoms of the coordinated H_2 molecule at 1.68 and 1.72 Å. An IRC study showed that TS(TT) connects with DHB1 and also with DHB2, thus supporting its role as transition state in the H/D exchange. In this way a "tick-tock" (TT) mechanism can be proposed for the experimentally observed proton−hydride exchange in such a way that the methoxy group could trap either the previously transferred proton to give DHB1 or the hydride to give DHB2. This "tick-tock" mechanism has been previously considered for the H/H exchange in Re hydride derivatives and theoretically supported by EHT calculations.[50] The relatively high barrier for this transition state, which is 35.4 kcal mol^{-1} from DHB2, points to a slow chemical transformation which fits with the slow H/D exchange experimentally observed.

In order to support the experimentally observed deuterium labeling of H_2 (blue dotted line in Chart 5), the structure HydOMe + H_2 was calculated. This fundamental state, modeling the loss of H_2 from DHB2 or from DHB1, is a monohydride−methoxy derivative that is 10.5 kcal mol^{-1} more stable than DHB2 and 5.4 kcal mol^{-1} more stable than DHB1. Unfortunately, we were not able to locate a transition state between HydOMe + H_2 and any of the two dihydrogen-bonded derivatives, but the connection between dihydrogen-bonded complexes and the corresponding product of the dihydrogen release can be considered as a reasonable reaction pathway.

In accord with the reaction coordinate discussed in the previous paragraphs, two related catalytic cycles can be proposed for the H/D exchange and the deuterium labeling of H_2 (Chart 6, red and blue cycles, respectively). In the first step of these catalytic cycles, from [Ru]-H, the participation of an intermediate of type HB (see Chart 5) is reasonable in the case of compounds bearing nitrogenated phosphines.

Chart 6. Proposed Catalytic Cycles for the H/D Exchange (Red, Left) or Deuterium Labeling of H_2 (Blue, Right)

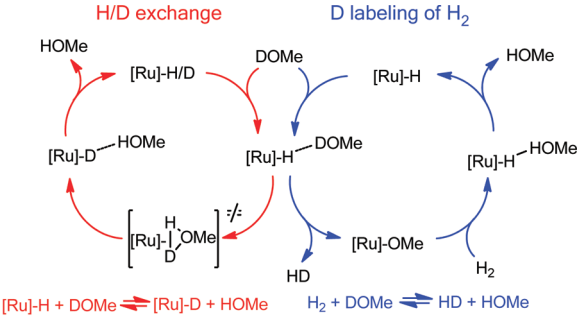

Addition of CF_3CO_2H to 2d. Finally, in order to assess whether the previous results are general or depend on the properties of the acid employed, we analyzed the effect of the addition of trifluoroacetic acid to compound **2d**. CF_3CO_2H is a weaker acid than HBF_4, but its anion has considerably higher coordination ability.

The proton transfer process that takes place after the addition, in an NMR tube, of an equimolar amount of CF_3CO_2H to a solution of **2d** in acetone-d_6, precooled to −90 °C, was monitored by ^1H and $^{31}P\{^1H\}$ NMR spectroscopy. The temperature was slowly increased from −90 to +20 °C (Figure 4). Initially, at −90 °C the proton acceptor is the basic nitrogen atom in the pyridine moiety, and this gives rise to the cationic derivative **3e**, $[RuH_2(\eta^6\text{-}p\text{-cymene})(\kappa^1P\text{-}PPh_2pyH)][CF_3CO_2]$

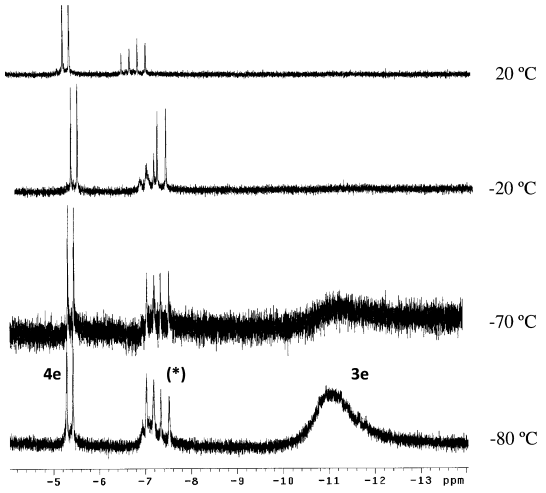

Figure 4. Evolution with temperature of the ^1H NMR hydride resonances of **3e** and **4e**. Resonances labeled with asterisks can be considered as being due to possible intermediates.

Chart 7. Mechanism Proposed for the Protonation of 2d with CF_3CO_2H To Give 3e and Subsequent Evolution to 4e, upon Increasing the Temperature, with Concomitant H_2 Loss

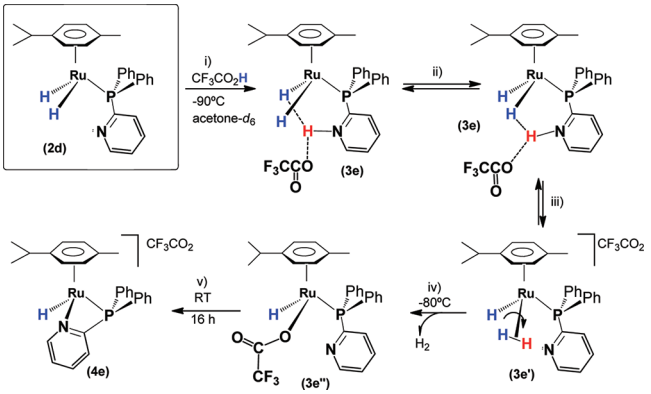

(Chart 7, step i). The $^{31}P\{^1H\}$ NMR spectrum at this temperature showed a single singlet at 80.08 ppm, whereas the most salient spectroscopic features in the ^1H NMR spectrum of this compound are the low-field broad resonance at 20.40 ppm, which integrates for one proton and is assigned to the N−H group, and the high-field broad signal at −11.08 ppm (integration for 2H), which corresponds to the hydride atoms. It is noteworthy that the position of the resonances of **3e** is not the same as in **3d** and there is a marked difference in the N−H signal (of around 8 ppm). This finding points to an interaction between the anion and the N−H group. In fact, the high chemical shift of the N−H group suggests the existence of a bifurcated dihydrogen bond, where the second basic center, in addition to the N atom, would be the $CF_3CO_2^-$ anion. A similar dihydrogen-bonded compound has been previously identified by our group.[18a] Considering that both the N−H and hydride signals are broad even at −90 °C, it is proposed that the hydride−proton interaction is dynamic and involves both hydride groups (Chart 7, step ii).

When the temperature is increased, both signals undergo significant broadening, a change that is consistent with the exchange process between the three hydrogen atoms. The interchange between these atoms was confirmed by a magnetization

dx.doi.org/10.1021/om300015j | Organometallics 2012, 31, 3087−3100

transfer observed between the two resonances. Even though it has not been observed, a nonclassical dihydrogen intermediate is proposed to take part in such a phenomenon (**3e′** in Chart 7, step iii). At −80 °C the loss of dihydrogen starts, a fact that implies a stability difference between **3e** and **3d**, since this loss was not observed until room temperature in the case of **3d**. From this temperature on, new signals in both the ^{1}H and the $^{31}P\{^{1}H\}$ NMR spectra appeared and these were assigned to the new monohydride **4e**, $[RuH(\eta^6\text{-}p\text{-cymene})(\kappa^2\text{-}P,N\text{-}PPh_2py)][CF_3CO_2]$, the spectroscopic data for which are nearly identical with those of **4d**.

We propose that the higher coordinating ability of the $CF_3CO_2^-$ anion, compared to that of BF_4^-, is the reason for the lower stability of the dihydrogen species in this system compared to that of **3d**. The anion could displace more easily the coordinated H_2 molecule.[51] As a matter of fact, additional peaks were found during the evolution with temperature in both the $^{31}P\{^{1}H\}$ NMR spectrum (at 20 °C: 56.90 (s) and 62.17 (s) ppm) and in the high-field region of the ^{1}H NMR spectrum (at 20 °C: −6.54 ppm (d, $^{2}J_{HP}$ = 52.4 Hz) and −6.88 ppm (d, $^{2}J_{HP}$ = 52.4 Hz)). These resonances could correspond to two additional monohydrides. One proposal is **3e″** (see Chart 7, step iv), although the solvent (acetone-d_6) could play a similar role in the stabilization of a monohydride species. These signals finally disappear when the sample is kept at room temperature for 16 h, leaving **4e** as the only detectable species.

CONCLUSIONS

In this work the protonation processes of arene Ru derivatives of the type $[RuH_2(arene)(PPh_2Het)]$ (arene = *p*-cymene, benzene; Het = 2-pyridyl (PPh_2py), 2-*N*-methylimidazolyl (dpim)) containing an uncoordinated N atom were studied both by experiments and with the help of theoretical calculations. The behavior of these compounds was compared with that of the derivatives $[RuH_2(arene)(PR_3)]$.

In the case of the protonation with HBF_4, at low temperature the N atoms are protonated first and a proton−hydride exchange is present. At room temperature the formation of monohydride species is observed. It was concluded that the species $[RuH_3(arene)(PPh_2Het)]BF_4$, which are formed as intermediates after the proton transfer, have a dual character as classical and nonclassical hydrides, with the nonclassical species being more stable, especially when Het = 2-pyridyl. This conclusion was based on the following facts: (i) the easy release of H_2 at room temperature with the concomitant coordination of the nitrogen atom; (ii) the low T_1 values measured; (iii) the results of calculations, which show that the nonclassical hydrides can access the slightly less stable classical species through energetically accessible transition states. Calculations performed for the species containing PPh_3 also reflect the dual character, and in our opinion the nature of this trihydride species might be reformulated as a consequence.

The role played by the uncoordinated N center is particularly relevant, as it interacts in all of the calculated structures with the transferred hydrogen atom. More importantly, in the $RuH(H_2)^+$ and the RuH_3^+ intermediates, this interaction makes the central hydrogen atom more electrophilic and thus favors the stabilization of the nonclassical species and the hydride−dihydrogen exchange.

The derivatives $[RuH_2(p\text{-cymene})(L)]$ (L = PPh_2py, dpim, PPh_3) were active catalysts for the H/D exchange of the hydride ligands with methanol-d_4. The process was faster for the complexes with PPh_2py or PPh_3. It was found that these derivatives were extremely active in H_2 labeling processes to give D_2 at room temperature (quantitative transformation in several minutes), with the OD of methanol-d_4 as the deuterium source. Mechanistic proposals for this transformation have been presented, and they are theoretically supported by a reaction coordinate that includes a "tick-tock" mechanism for the H/D exchange and the reversible loss of H_2. The presence of the uncoordinated nitrogen atom is not necessary for these catalytic processes to occur.

When an acid containing a counteranion with a higher coordinating ability (such as CF_3CO_2H) is used, the initial protonation of the N atom and the proton−hydride exchange also take place. In this case, however, a lower stability for the dihydrogen species was found, possibly because the H_2 molecule is more easily replaced by this anion.

EXPERIMENTAL SECTION

General Comments. All reactions were carried out under nitrogen using standard Schlenk techniques. Solvents were freshly distilled from convenient drying agents and degassed under nitrogen prior to use.

dpim,[52] PPh_2py,[53] $[RuCl_2(\eta^6\text{-arene})(\kappa^1P\text{-dpim})]$[22] (arene = *p*-cymene (**1b**), benzene (**1c**)), and $[RuCl_2(\eta^6\text{-}p\text{-cymene})(\kappa^1P\text{-}PPh_2py)]$ (**1d**)[54] were prepared according to previous procedures. $[RuH_2(\eta^6\text{-}p\text{-cymene})(\kappa^1\text{-}P\text{-}PPh_3)]$ (**2a**) was prepared by a procedure similar to that described for **2b−d**. $RuCl_3{\cdot}xH_2O$, PPh_3, HBF_4, and CF_3CO_2H were purchased from Aldrich.

NMR spectra were recorded on a Varian Unity Inova-400 (400 MHz for ^{1}H; 161.9 MHz for ^{31}P; 100.6 MHz for ^{13}C), a Varian UNITY-300 (300 MHz for ^{1}H; 121.4 MHz for ^{31}P; 75.4 MHz for ^{13}C) or a Varian Unity Inova-500 spectrometer (500 MHz for ^{1}H; 202,4 MHz for ^{31}P; 125.8 MHz for ^{13}C). Chemical shift values are reported in ppm. ^{1}H chemical shifts were recorded using the residual proton of the solvent as internal standard. Coupling constants (J) are in hertz. See Chart 8 for atom numbering. All ^{31}P chemical shifts were referenced internally. For the variable-temperature spectra the temperature of the probe (±0.1 K) was controlled by a standard unit calibrated with a methanol reference. Longitudinal relaxation time (T_1) measurements were made by the inversion-recovery method. In the NMR data, s, d, t, b, spt, o, m, and p refer to singlet, doublet, triplet, broad, septet, ortho, meta, and para, respectively. IR spectra were recorded on a Nicolet Impact 410 spectrophotometer as KBr pellets or on a Perkin-Elmer 883 (4000−200 cm^{-1} range) as Nujol mulls deposited on a polyethylene film.

Ab initio calculations were performed using the Gaussian 03 revision C.02 series of programs.[55] Density functional theory (DFT) was applied with the three-parameter hybrid functional of Becke and the Lee, Yang, and Parr correlation functional, more widely known as B3LYP.[56] The bulk effect of the solvent has been introduced through the PCM[57,58] continuum model by single-point calculations on gas-phase optimized geometries with default parameters for acetone as the solvent (ε = 20.7) to define the cavity in this model. The G_{solv} values

Chart 8. Atom Numbering for the *p*-Cymene Ring and Imidazolyl and Pyridyl Heterocycles

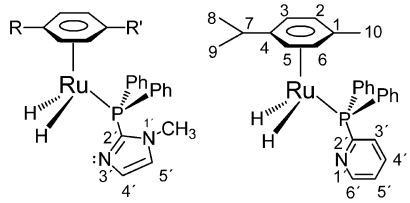

R=^{i}Pr; R′=Me, **2b**
R=H; R′=H, **2c**

2d

dx.doi.org/10.1021/om300015j | *Organometallics* 2012, 31, 3087−3100

account for the total free energy in solution with all non-electrostatic terms and the thermal correction to the Gibbs free energy in gas phase. For more computational details see the Supporting Information.

Synthesis of Complexes. *Preparation of [RuH_2(p-cymene)-(κ^1P-dpim)] (**2b**).* [$RuCl_2$(*p*-cymene)(dpim)] (**1b**; 109.5 mg, 0.19 mmol) was dissolved in ethanol (35 mL) to give an orange solution. KBH_4 (103 mg, 1.9 mmol) (molar ratio 1:10) was added, and a vacuum was applied as hydrogen was released during the reaction. The mixture became darker in a few minutes and was stirred at room temperature for 7 h. The resulting suspension was filtered to remove the additional KBH_4. A dark brown solution was obtained, and the solvent was evaporated under vacuum to afford a solid, which was extracted with n-pentane (3 × 15 mL). The liquid phase was filtered. The solvent of the resulting brown solution was evaporated under vacuum to dryness to give compound **2b**. The product is soluble in *n*-pentane, acetone, and ethanol. Yield: 28.7 mg (0.06 mmol), 35%. Anal. Calcd for $C_{26}H_{31}N_2PRu$: C, 61.99; H, 6.16; N, 5.56. Found: C, 62.23; H, 6.13; N, 5.7. ^{1}H NMR (400 MHz, acetone-d_6, room temperature): 7.86−7.76 (m, 4H, H^o-Ph); 7.36−7.24 (m, 6H, H^{m,p}-Ph); 7.15 (m, 1H, H$^{5'}$-Im); 6.95 (m, 1H, H$^{4'}$-Im); 5.28 (d, J_{HH} = 5.8 Hz, 2H, H^{3,5}-cym); 5.14 (d, J_{HH} = 5.2 Hz, 2H, H^{2,6}-cym); 3.51 (s, 3H, N-Me); 2.37 (spt, $^3J_{HH}$ = 6.9 Hz, 1H, H^7-cym); 1.65 (s, 3H, H^{10}-cym); 1.18 (d, $^3J_{HH}$ = 6.9 Hz, 6H, H^{8,9}-cym); −10.62 (d, $^2J_{PH}$ = 43.5 Hz, 2H, RuH_2) ppm. ^{13}C{^{1}H} NMR (100.577 MHz, acetone-d_6, room temperature): 147.9 (d, $^1J_{PC}$ = 68.4 Hz, 1C, C$^{2'}$-Im); 140.1 (d, $^1J_{PC}$ = 49.2 Hz, 2C, C^{ipso}-Ph); 133.98 (d, $^2J_{PC}$ = 12.7 Hz, 4C, C^o-Ph); 129.13 (d, $^4J_{PC}$ = 2.2 Hz, 2C, C^p-Ph); 127.6 (d, $^3J_{PC}$ = 10.5 Hz, 1C, C$^{4'}$-Im); 127.3 (d, $^3J_{PC}$ = 9.8 Hz, 4C, C^m-Ph); 124.4 (s, 1C, C$^{5'}$-Im); 112 (d, J_{PC} = 5.3 Hz, 1C, C^4-cym); 101.5 (s, 1C, C^1-cym); 87.5 (d, J_{PC} = 1.6 Hz, 2C, C^{3,5}-cym); 82.9 (d, J_{PC} = 3.5 Hz, 2C, C^{2,6}-cym); 34.8 (d, $^3J_{PC}$ = 2.3 Hz, 1C, N-Me); 32.3 (s, 1C, C^7-cym); 24.1 (s, 2C, C^{8,9}-cym); 5.1 (s, 1C, C^{10}-cym) ppm. ^{31}P{^{1}H} NMR (161.923 MHz, acetone-d_6, room temperature): 52.1 (s) ppm.

*Preparation of [RuH_2(benzene)(κ^1P-dpim)] (**2c**).* This compound was prepared as described for **2b** using 82.5 mg (0.16 mmol) of [$RuCl_2$(benzene)dpim] (**1c**) and 86.2 mg (1.6 mmol) of KBH_4 (molar ratio 1:10). Yield: 10.7 mg (0.024 mmol), 15%. *Pm* ($C_{22}H_{23}N_2PRu$): 447.26 g/mol. Analytical data for $C_{22}H_{23}N_2PRu$ are not available. The compound is very air-sensitive. ^{1}H NMR (400 MHz, acetone-d_6, room temperature): 8−7.1 (m, 12H, Ph, H$^{5',4'}$-Im); 5.21 (d, J_{PH} = 0.9 Hz, 6H, C_6H_6); 3.5 (s, 3H, N−Me); −10.35 (d, $^2J_{PH}$ = 40.6 Hz, 2H, RuH_2) ppm. ^{13}C{^{1}H} NMR: not available, compound hardly soluble. ^{31}P{^{1}H} NMR (161.923 MHz, acetone-d_6, room temperature): 51.1 (s) ppm.

*Preparation of [RuH_2(p-cymene)(κ^1-P-PPh_2py)] (**2d**). Method 1.* [$RuCl_2$(*p*-cymene)(PPh_2py)] (**1d**; 125 mg, 0.22 mmol) was dissolved in THF (20 mL) and $LiAlH_4$ (84 mg, 2.2 mmol) (molar ratio 1:10). The solution was stirred for 4 h at room temperature. The resulting yellow solution was purified by column chromatography (using Al_2O_3, 50−200 μm, and toluene/diethyl ether (1/1) in a 14 cm column). The solvent of the resulting brown solution was evaporated under vacuum until dryness and compound **2d** was obtained. Yield: 48.4 mg (0.10 mmol), 45%.

Method 2. This compound was also prepared as described for **2b** using 109.5 mg (0.19 mmol) of [$RuCl_2$(*p*-cymene)(PPh_2py)] (**1c**) and 103 mg (1.9 mmol) of KBH_4 (molar ratio 1:10). Yield: 60.3 mg (0.12 mmol), 65%. Anal. Calcd for $C_{27}H_{30}NPRu$: C, 64,78; H, 6.04; N, 2.79. Found: C, 64.60; H, 5.86; N, 2.69. ^{1}H NMR (300 MHz, acetone-d_6, room temperature): 8.12 (d, J_{HH} = 4.7 Hz, 1H, CH-py); 7.74(t, J_{HH} = 8.0 Hz, 4H, H^o-Ph); 6.81 (t, J_{HH} = 7.3 Hz, 4H, H^m-Ph); 6.73 (t, J_{HH} = 9.0 Hz, 2H, H^p-Ph); 6.62 (m, 1H, CH-py); 6.16 (m, 1H, CH-py); 5.24 (4H, CH-cym); 2.33 (spt, $^3J_{HH}$ = 7.0 Hz, 1H, H^7-cym); 1.84 (s, 3H, H^{10}-cym); 1.21 (d, $^3J_{HH}$ = 7.0 Hz, 6H, H^{8,9}-cym); −10.61 (d, $^2J_{PH}$ = 3.6 Hz, 2H, RuH_2) ppm. ^{13}C{^{1}H} NMR (75.4 MHz, acetone-d_6, room temperature): 148.70 (d, J = 12.5 Hz, 1C, py); 136.73 (d, J = 8.5 Hz, 1C, py); 134.05 (d, $^2J_{PC}$ = 11.5 Hz, 4C, C^o-Ph); 131.93 (d, J = 4.5 Hz, 1C, py); 128.74 (d, $^4J_{PC}$ = 2.5 Hz, 2C, C^p-Ph); 127.20 (d, $^3J_{PC}$ = 9.5 Hz, 4C, C^m-Ph); 122.73 (s, 1C, py); 109.98 (s, 1C, C^4-cym); 101.5 (s, 1C, C^1-cym); 87.24 (d, J_{PC} = 3.5 Hz, 2C, C^{3,5}-cym); 82.79 (d, J_{PC} = 4.0 Hz, 2C, C^{2,6}-cym); 31.05 (s, 1C, C^7-cym); 22.00 (s, 2C, C^{8,9}-cym); 19.50 (s, 1C, C^{10}-cym) ppm. ^{31}P{^{1}H} NMR (121.4 MHz, acetone-d_6, room temperature): 71.0 (s) ppm.

Protonation Experiments: Formation of Trihydrides and Monohydrides. Protonation experiments were carried out in 5 mm NMR tubes. Samples were prepared under nitrogen. In a typical experiment, 15−20 mg of dihydride **2b** was dissolved in 0.5 mL of CD_3COCD_3 and the tube was cooled to 183 K. $HBF_4{\cdot}OEt_2$ or CF_3CO_2H (1 equiv) was added using a microsyringe. The tube was shaken to mix all the reactants and then was immediately introduced into the probe at 183 K. ^{1}H and ^{31}P NMR spectra as well as T_1 measurements were carried out at this temperature and then at intervals of 20 K up to 298 K.

Deuteration Experiments. Deuteration experiments were carried out in 5 mm NMR tubes. Samples were prepared under nitrogen. In a typical experiment, 15−20 mg of dihydride **2b** was dissolved in 0.5 mL of CD_3OD, and the evolution of the reaction was monitored by ^{1}H NMR spectroscopy over a range of times. For the experiments with H_2, the gas was bubbled through the deuterated solution for 2 min and the NMR tube was then sealed with a Young valve under an H_2 atmosphere. The NMR spectra were recorded.

■ ASSOCIATED CONTENT

Ⓢ Supporting Information

Text, figures, and tables giving energies and selection of structural parameters for structures deduced from calculations, Mulliken charges calculated for some of these structures, and information on labeling processes. This material is available free of charge via the Internet at http://pubs.acs.org.

■ AUTHOR INFORMATION

Corresponding Author

*E-mail: Felix.Jalon@uclm.es. Fax: (+34) 926295318. Tel: (+34) 926295300.

Notes

The authors declare no competing financial interest.

■ ACKNOWLEDGMENTS

This work was supported by the MICINN of Spain (projects CTQ2011-24434 and CTQ2008-02403/BQU), the Junta de Comunidades de Castilla-La Mancha-FEDER Funds (PEII11-0214), and "Generalitat de Catalunya" (project 2009SGR409).

■ DEDICATION

Dedicated to Francisco Urbanos *in memoriam*.

■ REFERENCES

(1) (a) Besora, M.; Lledós, A.; Maseras, F. *Chem. Soc. Rev.* **2009**, *38*, 957−966. (b) Kubas, G. J. *Chem. Rev.* **2007**, *107*, 4152−4205. (c) Papish, E. T.; Magee, M. P.; Norton, J. R. In *Recent Advances in Hydride Chemistry*; Peruzzini, M., Poli, R., Eds.; Wiley: Amsterdam, 2001; pp 39−74.

(2) (a) Werner, H.; Kletzin, H. *J. Organomet. Chem.* **1983**, *243*, C59−C62. (b) Heinekey, D. M. *J. Am. Chem. Soc.* **1991**, *113*, 6074−6077. (c) Bergman, R. G.; Gilbert, T. M. *J. Am. Chem. Soc.* **1985**, *107*, 3502−3507. (d) Heinekey, D. M.; Millar, J. M.; Koetzle, T. F.; Payne, N. G.; Zilm, K. W. *J. Am. Chem. Soc.* **1990**, *112*, 909−919.

(3) (a) Crabtree, R. H.; Lavin, M. *J. Chem. Soc., Chem. Commun.* **1985**, 794−795. (b) Morris, R. H.; Sawyer, J. F.; Shiralian, M.; Zubkowski, J. D. *J. Am. Chem. Soc.* **1985**, *107*, 5581−5582.

(4) Maseras, F.; Lledós, A.; Clot, E.; Eisenstein, O. *Chem. Rev.* **2000**, *100*, 601−636.

(5) Jessop, Ph. G.; Morris, R. H. *Coord. Chem. Rev.* **1992**, *121*, 55−284.

(6) (a) Epstein, L. M.; Belkova, N. V.; Shubina, E. S. In *Recent Advances in Hydride Chemistry*; Peruzzini, M., Poli, R., Eds.; Wiley: Amsterdam, 2001; pp 391−418. (b) Belkova, N. V.; Epstein, L. M.; Shubina, E. S. *Eur. J. Inorg. Chem.* **2010**, 3555−3565.
(7) Chinn, M. S.; Heinekey, D. M. *J. Am. Chem. Soc.* **1987**, *109*, 5865−5867.
(8) Bakhmutov, V. I. *Dihydrogen Bonds: Principles, Experiments, And Applications*; Wiley: Amsterdam, 2008.
(9) Custelcean, R.; Jackson, J. E. *Chem. Rev.* **2001**, *101*, 1963−1980 and references therein.
(10) Epstein, L. M.; Shubina, E. S. *Coord. Chem. Rev.* **2002**, *231*, 165−181.
(11) (a) Belkova, N. V.; Besora, M.; Epstein, L.; Lledós, A.; Maseras, F.; Shubina, E. S. *J. Am. Chem. Soc.* **2003**, *125*, 7715−7725. (b) Belkova, N. V.; Collange, E.; Dub, P.; Epstein, L. M.; Lemenovskii, D. A.; Lledós, A.; Maresca, O.; Maseras, F.; Poli, R.; Revin, P. O.; Shubina, E. S.; Vorontsov, E. V. *Chem. Eur. J.* **2005**, *11*, 873−888. (c) Basallote, M. G.; Besora, M.; Castillo, C. E.; Fernández-Trujillo, M. J.; Lledós, A.; Maseras, F.; Máñez, M. A. *J. Am. Chem. Soc.* **2007**, *129*, 6608−6618. (d) Dub, P. A.; Filippov, O. A.; Belkova, N. V.; Daran, J.-C.; Epstein, L. M.; Poli, R; Shubina, E. S. *Dalton Trans.* **2010**, *39*, 2008−2015.
(12) Cf. the seminal work of Kubas: Kubas, G. J. *J. Chem Soc., Chem. Commun.* **1980**, 61−62 and many other examples in ref 1b.
(13) Clapham, S. E.; Hadzovic, A.; Morris, R. H. *Coord. Chem. Rev.* **2004**, *204*, 2201−2237.
(14) Bullock, R. M. *Angew. Chem., Int. Ed.* **2007**, *46*, 7360−7363.
(15) Laua, Ch. P.; Nga, S. M.; Jia, G.; Lin, Z. *Coord. Chem. Rev.* **2007**, *251*, 2223−2237.
(16) Heinekey, D. M.; Harper, T. G. P. *Organometallics* **1991**, *10*, 2891−2895.
(17) (a) Arliguie, T.; Border, C.; Chaudret, B.; Devillers, J.; Poilblanc, R. *Organometallics* **1989**, *8*, 1308−1314. (b) Limbach, H. H.; Ulrich, S.; Buntkowsky, G.; Sabo-Etienne, S.; Chaudret, B.; Kubas, G. J.; Eckert, J. *J. Am. Chem. Soc.* **1998**, *120*, 7929−7943. (c) Heinekey, D. M.; Payne, N. G.; Sofield, C. D. *Organometallics* **1990**, *9*, 2643−2645. (d) Gründemann, S.; Limbach, H. H.; Rodríguez, V.; Donnadieu, B.; Sabo-Etienne, S.; Chaudret, B. *Ber. Bunsen-Ges. Phys. Chem.* **1998**, *102*, 344−353.
(18) (a) Caballero, A.; Jalón, F. A.; Manzano, B. R. *Chem. Commun.* **1998**, 1879−1880. (b) Caballero, A.; Carrión, M. C.; Espino, G.; Jalón, F. A.; Manzano, B. R. *Polyhedron* **2003**, *23*, 361−371. (c) Jalón, F. A.; Manzano, B. R.; Caballero, A.; Carrión, M. C.; Santos, L.; Espino, G.; Moreno, M. *J. Am. Chem. Soc.* **2005**, *127*, 15364−15365.
(19) (a) Rossin, A.; Gonsalvi, L.; Phillips, A. D.; Maresca, O.; Lledós, A.; Peruzzini, M. *Organometallics* **2007**, *26*, 3289−3296. (b) Chu, H. S.; Lau, C. P.; Wong, K. Y.; Wong, W. T. *Organometallics* **1998**, *17*, 2768−2777.
(20) (a) Epstein, L. M.; Belkova, N. V.; Gutsul, E. I.; Shubina, E. S. *Pol. J. Chem.* **2003**, *77*, 1371−1383. (b) Belkova, N. V.; Epstein, L. M.; Shubina, E. S. *Eur. J. Inorg. Chem.* **2010**, 3555−3565.
(21) Jiménez-Tenorio, M.; Puerta, M. C.; Valerga, P.; Moncho, S.; Ujaque, G.; Lledós, A. *Inorg. Chem.* **2010**, *49*, 6035−6057.
(22) Caballero, A.; Jalón, F. A.; Manzano, B. R.; Espino, G.; Pérez-Manrique, M.; Mucientes, A.; Poblete, F. J.; Maestro, M. *Organometallics* **2004**, *23*, 5694−5706.
(23) Garrow, P. E. *Chem. Rev.* **1981**, *81*, 229−266.
(24) (a) Park, S. H.; Lough, A. J.; Yap, G. P. A.; Morris, R. H. *J. Organomet. Chem.* **2000**, *609*, 110−122. (b) Ayllon, J. A.; Sayers, S. F.; Sabo-Etienne, S.; Donnadieu, B.; Chaudret, B.; Clot, E. *Organometallics* **1999**, *18*, 3981−3990.
(25) Desrosiers, P. J.; Cai, L.; Richards, R.; Halpern, J. *J. Am. Chem. Soc.* **1991**, *113*, 4173−4184.
(26) Almeida, K.; Kranenburg, M.; Guari, Y.; Kamer, P. C. J.; van Leeuwen, P. W. N. M.; Sabo-Etienne, S.; Chaudret, B. *Inorg. Chem.* **2003**, *42*, 2859−2866.
(27) (a) Moreno, B.; Sabo-Etienne, S.; Chaudret, B.; Rodríguez-Fernández, A.; Jalón, F.; Trofimenko, S. *J. Am. Chem. Soc.* **1994**, *116*, 2635−2636. (b) Moreno, B.; Sabo-Etienne, S.; Chaudret, B.; Rodríguez-Fernández, A.; Jalón, F.; Trofimenko, S. *J. Am. Chem. Soc.* **1995**, *117*, 7441−7451. (c) Chen, Y. Z.; Chan, W. C.; Lau, C. P.; Chu, H. S.; Lee, H. L.; Jia, G. *Organometallics* **1997**, *16*, 1241−1246. (d) Morris, R. H. *Coord. Chem. Rev.* **2008**, *252*, 2381−2394.
(28) Werner, H.; Kletzin, H. *J. Organomet. Chem.* **1982**, *228*, 298−300.
(29) Bakhmutova, E. V.; Bakhmutov, V. I.; Belkova, N. V.; Besora, M.; Epstein, L. M.; Lledós, A.; Nikonov, G. I.; Shubina, E. S.; Tomas, J.; Vorontsov, E. V. *Chem. Eur. J.* **2004**, *10*, 661−671.
(30) Orlova, G.; Scheiner, S. *J. Phys. Chem. A* **1998**, *102*, 4813−4818.
(31) Belkova, N. V.; Besora, M.; Epstein, L. M.; Lledós, A.; Maseras, F.; Shubina, E. S. *J. Am. Chem. Soc.* **2003**, *125*, 7715−7725.
(32) Gusev, D. G. *J. Am. Chem. Soc.* **2004**, *126*, 14249−14257.
(33) Algarra, A. G.; Fernández-Trujillo, M. J.; Lledós, A.; Basallote, M. G. *Chem. Commun.* **2009**, *30*, 4563−4565.
(34) (a) Van Der Sluys, L. S.; Eckert, J.; Eisenstein, O.; Hall, J. H.; Huffman, J. C.; Jackson, S. A.; Koetzle, T. F.; Kubas, G. J.; Vergamini, Ph. J.; Caulton, K. J. *J. Am. Chem. Soc.* **1990**, *112*, 4831−4841. (b) Chaudret, B.; Chug, G.; Eisenstein, O.; Jackson, S. A.; Lahoz, F. J.; Lopez, J. A. *J. Am. Chem. Soc.* **1991**, *113*, 2314−2316. (c) Riehl, J.-F.; Pélissier, M.; Eisenstein, O. *Inorg. Chem.* **1992**, *31*, 3344−3345.
(35) (a) Maseras, F.; Durán, M.; Lledós, A.; Bertrán, J. *J. Am. Chem. Soc.* **1991**, *113*, 2879−2884. (b) Bianchini, C.; Masi, D.; Peruzzini, M.; Casarin, M.; Maccato, C.; Rizzi, G. A. *Inorg. Chem.* **1997**, *36*, 1061−1069. (c) Trovitch, R. J.; Lobkovsky, E.; Chirik, P. J. *Inorg. Chem.* **2006**, *45*, 7252−7260.
(36) Crabtree, R. H.; Lavin, M.; Bonneviot, L. *J. Am. Chem. Soc.* **1986**, *108*, 4032−4037.
(37) (a) Sabo-Etienne, S.; Chaudret, B. *Chem. Rev.* **1998**, *98*, 2077−2091. (b) McGrady, G. S.; Guilera, G. *Chem. Soc. Rev.* **2003**, *32*, 383−392. (c) Maseras, F.; Lledós, A.; Clot, E.; Eisenstein, O. *Chem. Rev.* **2000**, *100*, 601−636.
(38) (a) Zilm, K. W.; Heinekey, D. M.; Millar, J. M.; Payne, N. G.; Demou, P. *J. Am. Chem. Soc.* **1989**, *111*, 3088−3089. (b) Zilm, K. W.; Heinekey, D. M.; Millar, J. M.; Payne, N. G.; Neshyba, S. P.; Duchamps, J. C.; Szczyrba, J. *J. Am. Chem. Soc.* **1990**, *112*, 920−929. (c) Jones, D. H.; Labinger, J. A.; Weitekamp, D. P. *J. Am. Chem. Soc.* **1989**, *111*, 3087−3088.
(39) Limbach, H.-H.; Scherer, G.; Maurer, M.; Chaudret, B. *Angew. Chem., Int. Ed.* **1992**, *31*, 1369−1372.
(40) (a) Barthelat, J. C.; Chaudret, B.; Daudey, J. P.; De Loth, Ph.; Poilblanc, R. *J. Am. Chem. Soc.* **1991**, *113*, 9896−9898. (b) Jarid, A.; Moreno, M.; Lledós, A.; Lluch, J. D.; Bertran, J. *J. Am. Chem. Soc.* **1993**, *115*, 5861−5862. (c) Jarid, A.; Moreno, M.; Lledós, A.; Lluch, J. D.; Bertran, J. *J. Am. Chem. Soc.* **1995**, *117*, 1069−1075. (d) Camanyes, S.; Maseras, F.; Moreno, M.; Lledós, A.; Lluch, J. M.; Bertran, J. *J. Am. Chem. Soc.* **1996**, *118*, 4617−4621.
(41) Bondi, A. *J. Phys. Chem.* **1964**, *68*, 441−51.
(42) Basallote, M. G.; Besora, M.; Castillo, C. E.; Fernández-Trujillo, M. J.; Lledós, A.; Maseras, F.; Máñez, M. A. *J. Am. Chem. Soc.* **2007**, *129*, 6608−6618.
(43) Dub, P. A.; Belkova, N. V.; Filippov, O. A.; Daran, J.-C.; Epstein, L. M.; Lledós, A.; Shubina, E. S.; Poli, R. *Chem. Eur. J.* **2010**, *16*, 189−201.
(44) Baur, J.; Jacobsen, H.; Burger, P.; Artus, G.; Berke, H.; Dahlenburg, L. *Eur. J. Inorg. Chem.* **2000**, 1411−1422.
(45) Lough, A. J.; Park, S.; Ramachandran, R.; Morris, R. H. *J. Am. Chem. Soc.* **1994**, *116*, 8356−8357.
(46) (a) Caniguier, S.; Artero, V.; Fontecave, M. *Dalton Trans.* **2008**, 315−325. (b) Mealli, C.; Rauchfuss, T. B. *Angew. Chem., Int. Ed.* **2007**, *46*, 8942−8944.
(47) (a) Collman, J. P.; Wagenknecht, P. S.; Hembre, R. T.; Lewis, N. S. *J. Am. Chem. Soc.* **1990**, *112*, 1294−1295. (b) Heinen, A. V.; Papadogianakis, G.; Sheldon, R. A.; Peters, J. A.; van Bekkum, H. *J. Mol. Catal. A: Chem.* **1999**, *142*, 17−26. (c) Baba, A.; Nishikawa, M.; Eguchi, T. *J. Nucl. Mater.* **1997**, *250*, 29−35. (d) von Hahn, H. E. A.; Peters, E. *J. Phys. Chem.* **1971**, *75*, 571−579. (e) Grundler, P. V.; Yazyev, O. V.; Aebischer, N.; Helm, L.; Laurenczy, G.; Merbach, A. E. *Inorg. Chim. Acta* **2006**, *359*, 1795−1806. (f) Palibroda, N.; Grecu, E.;

Marginean, P. *Isotopenpraxis* **1986**, *22*, 435−438. (g) El-Nour, F. A.; Belacy, N.; Abdel-Khalik, M.; Khalil, T.; Aly, H. F. *Isotopenpraxis* **1990**, *26*, 529−531.
(48) Kurita, T.; Aoki, F.; Mizumoto, T.; Maejima, T.; Esaki, H.; Maegawa, T.; Monguchi, Y.; Sajiki, H. *Chem. Eur. J.* **2008**, *14*, 3371−3379.
(49) Himeda, Y.; Miyazawa, S.; Onozawa-Komatsizaki, N.; Hirose, T.; Kasuga, K. *Dalton Trans.* **2009**, 6286−6288.
(50) Feracin, S.; Buergi, T.; Bakhmutov, V. I.; Eremenko, I.; Vorontsov, E. V.; Vimenits, A. B.; Berke, H. *Organometallics* **1994**, *13*, 4194−4202.
(51) (a) Shubina, E. S.; Belkova, N. V.; Bakhmutova, E. V.; Vorontsov, E. V.; Bakhmutov, V. I.; Ionidis, A. V.; Bianchini, C.; Marvelli, L.; Peruzzini, M.; Epstein, L. M. *Inorg. Chim. Acta* **1998**, *280*, 302−307. (b) Belkova, N. V.; Ionidis, A. V.; Epstein, L. M.; Shubina, E. S.; Gruendemann, S.; Golubev, N. S.; Limbach, H.-H. *Eur. J. Inorg. Chem.* **2001**, 1753−1761. (c) Belkova, N. V.; Shubina, E. S.; Gutsul, E. I.; Epstein, L. M.; Eremenko, I. L.; Nefedov, S. E. *J. Organomet. Chem.* **2000**, *610*, 58−70.
(52) (a) Tolmachev, A. A.; Yurchenko, A. A.; Semenova, M. G.; Feshchenko, N. G. *Russ. J. Chem.* **1993**, *63*, 504−506. (b) Jalil, M. A.; Yamada, T.; Fujinami, S.; Honjo, T.; Nishikawa, H. *Polyhedron* **2001**, *20*, 627−633.
(53) Hintermann, L.; Dang, T.-Th.; Labonne, A.; Kribber, Th.; Xiao, L.; Naumov, P. *Chem. Eur. J.* **2009**, *15*, 7167−7179.
(54) Moldes, I.; Encarnación, E.; Ros, J.; Alvarez-Larena, A.; Piniella, J. F. *J. Organomet. Chem.* **1998**, *566*, 165−174.
(55) See ref 1 in the Supporting Information.
(56) (a) Becke, A. D. *J. Chem. Phys.* **1993**, *98*, 5648−5652. (b) Becke, A. D. *J. Chem. Phys.* **1992**, *96*, 2155−2160. (c) Lee., C.; Yang, W.; Parr, R. G. *Phys. Rev.* **1988**, *B37*, 785−789. (d) Ditchfield, R.; Hehre, W. J.; Pople, J. A. *J. Chem. Phys.* **1971**, *54*, 724−728. (e) Ditchfield, R.; Hehre, W. J.; Pople, J. A. *J. Chem. Phys.* **1972**, *56*, 2257−2260. (f) Hariharan, P. C.; Pople, J. A. *Mol. Phys.* **1974**, *27*, 209−214. (g) Gordon, M. S. *Chem. Phys. Lett.* **1980**, *76*, 163−168. (h) Clark, T.; Chandrasekhar, J.; Spitznagel, G. W.; Schleyer, P. v. R. *J. Comput. Chem.* **1983**, *4*, 294−301.
(57) Foresman, J. B.; Keinth, T. A.; Wiberg, K. B.; Snoonian, J.; Frisch, M. J. *J. Phys. Chem.* **1996**, *100*, 16098−16104.
(58) Cossi, M.; Barone, V. *J. Chem. Phys.* **2001**, *115*, 4708−4718.